

Journal Pre-proofs

Immediate-released pelletized solid dispersion containing fenofibrate: formulation, *in vitro* characterization, and bioequivalence studies in experimental beagle dogs

Chien Ngoc Nguyen, Cuong Viet Pham, Giap Le Thien, Bao Tran Ngoc, Ha Le Thi, Chang Pham Thi Huyen, Thuan Nguyen Thi

PII: S0378-5173(19)30706-9
DOI: <https://doi.org/10.1016/j.ijpharm.2019.118661>
Reference: IJP 118661

To appear in: *International Journal of Pharmaceutics*

Received Date: 1 May 2019
Revised Date: 30 August 2019
Accepted Date: 2 September 2019

Please cite this article as: C.N. Nguyen, C.V. Pham, G. Le Thien, B.T. Ngoc, H. Le Thi, C.P.T. Huyen, T.N. Thi, Immediate-released pelletized solid dispersion containing fenofibrate: formulation, *in vitro* characterization, and bioequivalence studies in experimental beagle dogs, *International Journal of Pharmaceutics* (2019), doi: <https://doi.org/10.1016/j.ijpharm.2019.118661>

This is a PDF file of an article that has undergone enhancements after acceptance, such as the addition of a cover page and metadata, and formatting for readability, but it is not yet the definitive version of record. This version will undergo additional copyediting, typesetting and review before it is published in its final form, but we are providing this version to give early visibility of the article. Please note that, during the production process, errors may be discovered which could affect the content, and all legal disclaimers that apply to the journal pertain.

© 2019 Published by Elsevier B.V.



Immediate-released pelletized solid dispersion containing fenofibrate: formulation, *in vitro* characterization, and bioequivalence studies in experimental beagle dogs.

Chien Ngoc Nguyen^{1,2*}, Cuong Viet Pham², Giap Le Thien³, Bao Tran Ngoc¹, Ha Le Thi⁴, Chang Pham Thi Huyen⁵, Thuan Nguyen Thi⁶

¹ Department of Pharmaceutical Industry, Hanoi University of Pharmacy, Hanoi, Vietnam

² National Institute of Pharmaceutical Technology, Hanoi University of Pharmacy, Hanoi, Vietnam

³ Student K67, Department of Pharmaceutical Industry, Hanoi University of Pharmacy, Hanoi, Vietnam

⁴ Master student CH22, Hanoi University of Pharmacy, Hanoi, Vietnam

⁵ Master student CH21, Hanoi University of Pharmacy, Hanoi, Vietnam

⁶ Department of Pharmaceutical Chemistry, Hanoi University of Pharmacy, Hanoi, Vietnam

*The corresponding author.

*Corresponding author: Chien Ngoc Nguyen

Postal address: Hanoi University of Pharmacy, 13-15 Le Thanh Tong street, Hoan Kiem district, Hanoi, Vietnam

E-mail: nguyennngocchien@yahoo.com, chiennn@hup.edu.vn

Abstract

There have been many strategies to increase solubility, dissolution rates, and oral bioavailability of fenofibrate such as micronization, nanonization, solid dispersion, and emulsion so far. To our knowledge, only first three technologies have been applied in producing marketed products, and no combination of solid dispersion and pellet has been found even in laboratory-based reports. Therefore, the aim of this study was to develop novel solid dispersion-based pellets via a one-step process directly from fenofibrate powder using layering method. Developed fenofibrate pellets were *in vitro* characterized on size distribution, dissolution rates, sensory evaluation and stability. In addition, the transformation from crystalline fenofibrate to amorphous fenofibrate, and intermolecular interactions of fenofibrate in solid dispersion were confirmed using physico-chemical methods. The dissolution rate of pellets containing fenofibrate was significantly higher than that of the reference, Lipanthyl® 160 mg tablets at early stage, satisfying the criteria in USP 38. The pellets, then, were packed in hard capsules for bioequivalence studies in experimental beagle dogs using a validated HPLC assay. Final findings of the present study should be beneficial for further development of new fenofibrate formulations containing solid dispersion-based pellets which were bioequivalent to Lipanthyl® 160 mg tablets.

Keywords: fenofibrate, pellets, layering, solid dispersion, bioequivalence study, pharmacokinetic study

1. Introduction

Fenofibrate (FB), a widely used dyslipidaemic drug, was firstly synthesized in 1974 as a member of fibrates (Fischer J., 2006; Guichard et al., 2000; Lalloyer and Staels, 2010). FB has some outstanding advantages compared to its derivatives, such as improved pharmacokinetic and pharmacological properties, greater decreases in total cholesterol and low-density lipoprotein cholesterol, and the ability of combination with other lipid-altering agents in treatment (Ballantyne, 2009; Lalloyer and Staels, 2010). The recent demonstration of valuable properties

on microvascular complications of diabetes mellitus with FB, has further consolidated the interest for the drug (Lalloyer and Staels, 2010; Qiu et al., 2019; Xin et al., 2019). However, FB is a lipophilic compound ($\log P = 5.24$) that is poorly water-soluble, making it challenging to consistently achieve therapeutic drug level (Adkins and Faulds, 1997; Ling et al., 2013; Ueda et al., 2019).

Direct challenges to solubility has encouraged the advancement of novel formulations containing FB planned to increase the oral bioavailability by means of several different approaches since its clinical use in the 1990s as standard preparation (Adkins and Faulds, 1997; Lalloyer and Staels, 2010). Many strategies such as micronization (Lipanthyl®, Antara®, Tricor®) (Hens et al., 2015; Li et al., 2019; Sironi et al., 2017; Vogt et al., 2008), nanoparticle technology (Tricor®, Triglide®, Lipidil 145 ONE®) (Ibrahim et al., 2018; Kumar and Siril, 2018; Sironi et al., 2017), solid dispersion technology (Fenoglide®) (Ibrahim et al., 2018; Pestieau et al., 2017; Sheu et al., 1994; Shi et al., 2019; Shi et al., 2017), and emulsifying technology (Alshamsan et al., 2018; Patki and Patel, 2019; Pestieau et al., 2017; Sunazuka et al., 2018) have been used to enhance the bioavailability of FB. Therein, solid dispersion has been considered as one of powerful approaches to increase the dissolution profiles of practically water-insoluble drugs (Vo et al., 2013). The advantages of solid dispersions are ascribed to the reduction of particle size which may reduce to the molecular level, transformation from crystalline state of the drug to amorphous state, the wettability and porosity enhancement, and enormous potential for commercial applications (Baghel et al., 2016; Ibrahim et al., 2018; Singh et al., 2011). Although the applications of micronization and nanonization technologies in current commercial products have reduced daily dose of FB from 100 mg of non-micronized FB to 67 mg of micronized FB (Lofibra®, Gate), and from 200 mg of micronized FB to 145 mg of nanocrystal FB (TriCor®, Abbott) (Ling et al., 2013), respectively, the large size of such tablets and the tendency towards aggregation of the drug in powder in the stomach upon dosing may cause longer time to reach the maximum plasma concentration (T_{max}) and gastrointestinal irritation. In this context, pellets can provide rapid onset of action and faster drug release due to the smaller size than tablets, widely homogeneous distribution and less residence time of drugs in the stomach (Patel and Gohel, 2019).

By taking advantages of these beneficial properties from solid dispersion and pellet to enhance the oral bioavailability of FB, the objective of this study was to develop FB immediate-released pellets satisfying not only the dissolution rate criteria in USP 38 ((NF), 2015) and pharmacokinetic parameters which are bioequivalent to those of Lipanthyl® 160 mg tablets (Abbott, USA) but also a shorter T_{max} . Additionally, even though fenofibric acid (FA) has been well known as a main active metabolite of FB after oral administration (Streel et al., 2000; Wang et al., 2012; Zhu et al., 2010), FB may exist as an unchanged form in plasma after oral administration of formulations in this study. Therefore, we also developed and validated a simple and rapid HPLC assay to measure FA and FB in beagle dog plasma for full evaluation of pharmacokinetics profiles.

2. Materials and Methods

2.1. Chemicals and reagents

FB was purchased from Zhejiang Excel Pharmaceutical Co., Ltd (China). Fenofibric acid (FA) was obtained from Selleck (U.S.A). Diclofenac sodium (internal standard, IS) was purchased from Sigma-Aldrich (Germany). Polyvinyl pyrrolidone K30 (PVP K30) was received from Hefei Trendchem Co., Ltd. (China). Hydroxyl propyl methyl cellulose E6 (HPMC E6) and hydroxyl propyl methyl cellulose E15 (HPMC E15) were obtained from Zhongbao Chemicals Co.,Ltd (China). Polyethylene glycol 6000 (PEG 6000) and polyethylene glycol 4000 (PEG 4000) were procured from Sino-Japan Chemical Co., Ltd (Taiwan). Eudragit® EPO was supported by Evonik Co., Ltd (Germany). Sodium lauryl sulfate (NaLS) was purchased from Samchun Pure Chemical Co., Ltd (Korea). Lutrol® F127 was provided by BASF SE (Germany). Tween 80 and Span 60 were obtained from Guangzhou Quanao Chemical Co., Ltd (China). Sugar spheres were purchased from Colorcon Pte Ltd (U.S.A). HPLC-grade methanol, acetonitrile was purchased from Fisher Scientific (U.S.A). All other reagents and solvents were of analytical grade and used without further purification.

2.2. Animals

Ten healthy male beagle dogs (between 10 kg and 12 kg in weight) were obtained Hanoi University of Pharmacy (Hanoi, Vietnam) for an *in vivo* study. The study protocol was approved

by the ethics committee of medicine and pharmacy research at Military Medical University, approval number: 024C/14, dated December 2nd, 2018.

2.3. Preparation of pelletized solid dispersion of FB

Firstly, 2.50 gram of FB was dissolved in 30 mL of dichloromethane, then 30 mL of absolute ethanol was added in the solution. Subsequently, polymer was completely dissolved in the solution of FB. Resulting solution was homogeneously mixed with desired amounts of surfactants before processed with 5 gram of sugar spheres in a Mini-Glatt fluidized-bed system (Glatt, Germany) (Table 1). The layering procedures were processed with parameters provided in Table 1. Final formulation (F19) was prepared for desirable amount of FB (160 mg) in capsule (Table 1) based on the development of formulation of FB pellets (from F1 to F18).

2.4. In vitro characterization of FB pellets

2.4.1. Size distribution of FB pellets and layering efficiency (LE)

Size distribution of FB pellets was measured using a set of meshes (mesh no.25, mesh no. 20, mesh no. 18, and mesh no. 16). Layering efficiency was calculated using the following equation:

$$LE = \frac{m_2 - m_1}{m_1} \times 100 (\%)$$

Where m_1 , m_2 were the weight of sugar cores and the weight of layered pellets in a range of mesh no. 20 and mesh no. 16, respectively.

2.4.2. In vitro dissolution test

Dissolution testing of FB pellets was conducted, in triplicate, by USP 38 apparatus 2 (paddle method) using a dissolution tester (Pharmatest, Germany, Model: PT-DT8S). Briefly, a sample of pellets (equivalent to 160 mg of FB) was placed into 900 mL of dissolution medium containing 0.72% NaLS or 0.40% NaLS at $37 \text{ }^\circ\text{C} \pm 0.5 \text{ }^\circ\text{C}$, under a stirring speed of 75 ± 2 rpm. At desired time points, 5 mL of samples were withdrawn through a One-micron Full Flow Filter, filtered through membranes $0.45\mu\text{m}$ (Sartorius, Germany, Model Minisart RC 25) then diluted 20 times with fresh medium before analyzed by a UV spectrophotometer (OPTIMA, Japan, Model: SP – 3000 Nano) at 291 nm. The medium was re-filled with 5 mL of fresh medium immediately after each time of withdrawing.

The similarity factor (f_2) was employed to compare dissolution profiles using the following equation (Li et al., 2019):

$$f_2 = 50 \times \log \left\{ \left[1 + \frac{1}{n} \sum_{i=1}^n (R_i - T_i)^2 \right]^{-0,5} \times 100 \right\}$$

Where: R_i : % dissolved FB of reference at time point i ($i = 1, n$)

T_i : % dissolved FB of test sample at time point i ($i = 1, n$)

If f_2 value is equal to or higher than 50, then the dissolution profiles are similarly considered. The similarity is greater when f_2 value is larger.

2.5. Characterization of FB solid dispersion

2.5.1. Powder X-ray diffraction (PXRD)

Developed pellets, FB materials, physical mixture and interested raw materials were separately milled into smooth powder using a mortar before was gently packed into sample holders. The study was conducted using an X-ray diffractometer (D8 Advance, Bruker, Karlsruhe, Germany) over a 2θ interval of 0° to 60.0° . The step size was $0.0375^\circ/s$, at 25°C .

2.5.2. Differential scanning calorimetry (DSC)

The phase transition of developed pellets, FB materials, physical mixture and interested raw materials were analyzed by differential scanning calorimeter (Mettler Toledo DSC 1, USA) at a heating rate of $10^\circ\text{C}/\text{min}$ from 0°C to 200°C , and an empty aluminum pan was used as a reference.

2.5.3. Fourier-transform infrared spectroscopy (FT-IR)

FT-IR spectra were obtained using a spectroscopy (JASCO FT/IR – 6700, Japan) over the region of $4000\text{--}400\text{ cm}^{-1}$. FB, FB pellets, and raw materials were milled into powder with KBr ($50\text{--}100\text{ mg}$), then compressed into the discs by applying a pressure of 10 tons for 1 min in a hydraulic press. Subsequently, the discs were placed in the light path for recording the spectra.

2.6. Stability of FB pellets in capsules

The amount of pellets containing approximately 160 mg of FB were packed in a capsule (hard gelatin capsule, size 0), then kept in tightly lidded, colourless glass vials, under an accelerated condition of a temperature of $40\text{ }^{\circ}\text{C} \pm 2\text{ }^{\circ}\text{C}/75\% \pm 5\%$ relative humidity for 1 month or a condition of $30\text{ }^{\circ}\text{C} \pm 2\text{ }^{\circ}\text{C}/75\% \pm 5\%$ relative humidity for 12 months using Daeyang ETS TH – 180S (Korea). The shape, color, the content of FB in pellets, and dissolution rates of FB in the medium of 0.4% NaLS were re-evaluated after different storages. In addition, any possibility of transformation of FB state and changes in molecular interactions of FB with other components in the pellets stored under the long-term condition for 12 months also investigated with PXRD, DSC, and FT-IR.

2.7. HPLC analysis

Developed HPLC analysis was carried out on a Shimadzu LC 20A (Japan). Elution of FA, FB, and diclofenac sodium (IS) were achieved using a gradient mobile phase of methanol and 0.01M phosphate buffer pH 3.0 (Table 2) at flow rate of 1.0 mL/min with the injection volume was 20 μL . An employed Shim-pack GIST C18 (150 x 4.6mm; 5 μm) column was maintained at 25 $^{\circ}\text{C}$, and samples were kept at 5 $^{\circ}\text{C}$. The signals of chromatograms were detected at 286 nm.

2.8. Plasma sample preparation

For standard samples, working solutions of FA and FB (5 $\mu\text{g}/\text{mL}$ and 50 $\mu\text{g}/\text{mL}$ in methanol) were prepared from stock solution (500 $\mu\text{g}/\text{mL}$ in methanol). Then desired volumes of these working solutions were completely evaporated in glass tubes under a gentle nitrogen stream at room temperature. Residues in these tubes were vortexed in 1000 μL of blank beagle dog plasma for 60 seconds before added with 100 μL of IS solution (100 $\mu\text{g}/\text{mL}$ of diclofenac sodium in methanol) and 500 μL of solution of saturated sodium chloride. The resulting mixture, subsequently, was shaken for 5 second. After that, an extraction process was performed by adding 5 mL of ethyl acetate into the mixture. The process of liquid-liquid extraction (LLE) was continually performed by horizontally shaking the obtained mixture for 15 minutes at a speed of 300 times per minute, then centrifuging the mixture at 5500 rpm for 20 minutes. After centrifuging, 3 mL of the upper layer was completely dried in glass tubes under a gentle nitrogen stream at room temperature. Finally, residues in these tubes were dissolved in 1000 μL of mobile

phase consist of methanol and 0.01M phosphate buffer pH 3.0 (70:30, v/v) prior to analyzing by HPLC.

For QC samples including lower quality control (LQC) sample, middle quality control (MQC) sample, and higher quality control (HQC) sample were processed in the same way detailed above.

For blank samples and animal samples, these samples were also prepared in a similar way above with the notice that only blank plasma (without FA and FB) was used for blank samples and only blood samples from pharmacokinetic study were involved in for animal samples.

2.9. HPLC method validation

The HPLC method utilized in this study was validated according to Bioanalytical Method Validation for Industry of FDA (FDA, 2018) including selectivity, carryover, calibration curves, linearity, limit of detection (LOD), lower limit of quantitation (LLOQ), extraction recovery, precision, accuracy, and stability for both of FA and FB. Selectivity was conducted with blank samples in six different sources of blank plasma, and standard samples of FA and FB at the lowest concentration of calibration curves and IS. Carryover was calculated by analyzing standard samples at LLOQ, then alternately analyzing standard samples at upper limitation of quantification (ULOQ) and blank samples. Linearity of the assay was examined based on the correlation between the ratio of analyte peak area/ IS peak area and concentration over six different concentrations of either FA or FB. Both LOD and LLOQ were calculated when the signal-to-noise ratios were 3 and 5 over a set of standard samples, respectively. The intra-day (single day) and inter-day (three consecutive days) precisions and accuracies of FA and FB were verified by analyzing three (LQC, MQC, and HQC) standard samples six times. Recoveries of FA and FB after extraction were examined over two standard samples at LQC, and HQC. These samples were prepared in the method detailed above before analyzed by the HPLC method.

2.10. Pharmacokinetics studies

Beagle dogs in this study were housed in clean cages at a temperature of $25 \pm 2^\circ\text{C}$ with a 12-h light/dark cycle. Also, such cages were maintained at $55 \pm 5\%$ relative humidity in laminar flow. All these dogs were fed with only water and commercial diet, and were fasted for 24 hours prior to the study. This study was based on a single-dose, randomized, and two-period crossover design. In phase I, five dogs were randomly chosen and then each experimental dog was

administered a single dose of reference product (Lipanthyl® 160 mg tablet) with 100 mL of water. Five other dogs were administered a single dose of test product (one capsule with approximately 160 mg of FB) in the same way. Ten dogs were kept fasted until the first blood collection. Water was allowed after 4 hours of the administration. Then, phase II of the study was conducted 144 hours after completing phase I. The process of phase II was carried out inversely with respect to the animals and study products.

Blood samples (3.0 mL each time) were collected into heparinized tubes through sterile syringes from the jugular vein before (0 h) and at 0.5, 1.0, 1.5, 2.0, 3.0, 4.0, 5.0, 6.0, 7.0, 8.0, 10, 12 and 24 h after dosing. The blood samples, then, were centrifuged at 5000 rpm for 5 minutes. Afterwards, plasma was separated from serum and kept frozen at -30 °C within 30 days until further analysis.

2.11. Pharmacokinetic analysis

The concentration of FA (and/or FB) in the plasma was calculated from the peak area ratio of FA (and/or FB) to the IS, diclofenac sodium. Oral pharmacokinetic analysis was performed using a non-compartmental model with WinNonlin Professional 2.1 software (Pharsight, Mountain View, CA, USA) to produce pharmacokinetic parameters including area under the curve to the last measurable concentration (AUC_{0-t}), the maximum plasma concentration (C_{max}), and the time to reach the maximum plasma concentration (T_{max}) from experimental data. The area under the curve extrapolated to infinity ($AUC_{0-\infty}$) was calculated by the following formulation: $AUC_{0-\infty} = AUC_{0-t} + C_t/K_{el}$, where C_t is the last measurable concentration and K_{el} is the elimination rate constant (FDA, 2002). The half-life ($t_{1/2}$) was calculated as $0.693/K_{el}$. Relative bioavailability (R.B.) were calculated from AUC_{0-t} .

2.12. Statistical analysis and bioequivalence evaluation

All samples were measured at least triplicate. Data was expressed as mean \pm standard deviation (SD). Statistical significance was performed using one-way ANOVA and Student's *t*-test. Two compared parameters were statistically significant when *p*-value < 0.05.

Bioequivalence studies were performed with the consideration of log-transformed data of C_{max} , and AUC_{0-t} . The product was considered bioequivalent to reference if the difference

between two compared parameters was found statistically insignificant ($p \geq 0.05$) and 90 % confidence intervals for geometric mean ratios of test to reference product fell within 80.00 – 125.00% as the European Medicines Agency guidelines (EMA, 2010; Min et al., 2019).

3. Results and discussions

3.1. Development of FB pellet formulation

Hydrophilic carrier polymers play not only a pivotal role in preparing solid dispersions but also in pelletization by layering (Baghel et al., 2016; Singh et al., 2011). Hence, firstly we investigated some different polymers with careful consideration of pellet processing (F1-F4, Table 1).

Figure 1 summarizes characteristics of the pelletization process, and dissolution rates against different formulations with various polymers. Pellets only were successfully prepared using HPMC E6 or PVP K30, otherwise the filter or nozzle in the fluid bed system was blocked when FB was mixed with PEG 6000 (F3) or Eudragit® EPO (F4), respectively. For F3, the layering process was discontinued due to the clogging of the filter then the air could not enter the system (Figure 1A). This can be explained by low melting temperature of PEG 6000 (55 °C – 63 °C) (Raymond C. Rowe, 2009). With regard to F4, the glass transition temperature of Eudragit® EPO was around the inlet air temperature of the pelletization procedure, causing the polymer layer on the surface of the pellet viscous when increasing the inlet air temperatures (slightly higher than the glass transition temperature). On the other hand, the solvent slowly evaporated when reducing the inlet air temperature. Taken together, these made F4 pellets sticking in the chamber.

For F2, formed PVP K30 coating layer was quite sticky, and then limited the movement of pellets, decreasing the layering efficiency. This led to air flow reduction, but this reduction resulted in low layering efficiency (Figure 1A). Inversely, F1 pellets were layered in an easier way with higher layering efficiency.

In terms of dissolution test in 0.72% NaLS medium according to USP 38, corresponding amount of F1 pellets and F2 pellets containing approximately 160 mg of FB was employed. The dissolution profiles of FB in F1 and F2 were shown in Figure 1B and 1C. F1 pellets had higher dissolution rate ($99.85 \pm 0.68\%$ at 30-min point) in comparison with that of F2 ($76.42 \pm 2.79\%$ at

30-min point). The reason may be the hygroscopic property of solid dispersion prepared with PVP K30, probably triggering a rapid transformation from amorphous into crystalline of drug, then reducing the solubility of FB. Hence, the formulation of F1 was chosen for further development.

After choosing HPMC E6 as a main carrier in solid dispersion formulation, we investigated the effect of FB/HPMC E6 ratio (w/w) on the dissolution rate of FB in NaLS medium. Because no significant differences between dissolution rates of formulations containing different FB/HPMC E6 ratios (w/w) in 0.72% NaLS medium were found (data not shown), thus we reduced NaLS concentration to 0.40% for further evaluation. The strategy for selecting 0.4% NaLS medium was due to critical micelle concentration of NaLS (0.2365%) (Raymond C. Rowe, 2009) and the capacity of medium for differentiating the dissolution rates of FB in different formulations.

Figure 2A shows the dissolution profiles of FB in 0.4% NaLS medium from different formulations whose FB/HPMC E6 ratios (w/w) ranging from 1:0.5 (F5) to 1:2.0 (F7). The dissolution rates significantly increased from the ratio of 1:0.5 to 1:1, but kept similar at higher ratios. Hence, the FB/HPMC E6 ratio (w/w) of 1:1 was selected as an optimal FB/HPMC E6 ratio (w/w). Also, the data supported for the utilization of 0.4% NaLS medium in evaluating the effect of formulation factors on the dissolution rates of various FB pellets.

Although solid dispersion can increase the solubility of insoluble active ingredients, this approach inherently is not stable over a storage period due to state transformations of drug. Hence, with the purpose of increasing the stability of FB solid dispersion, NaLS, as a surfactant, was selected in preparing the solid dispersion (Weng et al., 2014; Zhu et al., 2011). Moreover, NaLS also may enhance the solubility of FB in solid dispersion.

Figure 2B shows dissolution profiles of FB in 0.4% NaLS medium from different formulations containing FB/NaLS ratios (w/w) ranging from 1:0.1 (F8) to 1:1.0 (F12). For first two ratios (1:0.1 and 1:0.2), the dissolution rates increased with the growth of NaLS amount in formulation ($75.13 \pm 0.42\%$, and $79.55 \pm 0.19\%$ at time point of 60 min, respectively). The reason possibly came from the more stable interactions between FB and polymer in presence of a surfactant, resulting in the better dispersion of FB in solid dispersion. Also, NaLS probably enhance the solubility of FB at the same time. Inversely, the rate kept unchanged when the ratio

over 1:0.2. This possibly was ascribed to no significant difference in the interactions in the solid dispersion. In the study of Wusheng Zhu and co-workers., it was proved that the interactions of the mixture including HPMC and NaLS with FB is the best among investigations, having a stable effect, reducing re-crystallization better than HPMC alone or HPMC and Tween 80 mixture (Zhu et al., 2011). Based on these results, F9 formulation with FB/NaLS ratio (w/w) of 1:0.2 was selected for further development. Once again, these results supported for the successful application of 0.4% NaLS medium in evaluating the effect of formulation factors on the dissolution rates of various FB solid dispersions in this study.

In order to continually strengthen the stability and dissolution rates of FB solid dispersion, we examined other carriers including Poloxamer 407 (F13), HPMC E15 (F14), Tween 80 (F15), Span 60 (F16), and PEG 4000 (F17) at the FB/carrier ratio (w/w) of 1:0.1.

Figure 2C shows the dissolution profiles of FB in 0.4% NaLS medium from different formulations prepared with above additional carriers. F14 showed the highest dissolution rate at time point of 60 minutes among six investigated formulations and significantly different to second one, F13. Additionally, when FB/HPMC E15 ratio (w/w) increased from 1:0.1 (F14) to 1:0.2 (F18), the dissolution rates remained similar for both formulations (Figure 2D). Hence, F14 was selected for a comparison between the dissolution rate of F14 and that of a reference product, Lipanthyl® 160 mg tablet.

Figure 3A and 3B show data on the dissolution profiles of F14 and Lipanthyl® 160 mg in 0.4% NaLS medium. At some first points, the dissolution rate of F14 was lower than that for the reference. However, the opposite was seen from time point of 30 minutes on. And at the end of profiles, significant difference in dissolution rates of two products was found, $81.60 \pm 1.43\%$ for F14 and $72.00 \pm 0.14\%$ for the reference. Also, data on size distribution indicated that over 99% of F14 pellets was within a range of mesh no. 16 and mesh no. 20 (Figure 3C). These findings revealed that F14 was suitable for preparing desired FB capsules.

According to the amount of layering solution employed, F19 formulation was then prepared with the FB content of 160mg packed in one hard capsule size 0 (Table 1).

3.2. Characterization of FB solid dispersion

3.2.1. Powder X-ray diffraction (PXRD)

PXRD patterns of FB material, F14 pellet, sugar sphere, NaLS and HPMC E6 were illustrated in Figure 4. From the results of PXRD, crystalline FB had its characteristic diffraction peaks at 11.86 °; 14.38 °; 16.61 °; 22.15 °; 26.17 ° and 36.72 °. HPMC E6 had no its characteristic peaks. Sugar sphere had its characteristic peaks at 18.9 °; 19.7 ° and 24.9 °. Only characteristic diffraction peaks of sugar sphere were clearly shown in the PXRD pattern of F14 pellet, while the characteristic diffraction peaks of FB decreased in both quantity and intensities. This suggested that FB in F14 pellet mainly existed in amorphous state.

3.2.2. Differential scanning calorimetry (DSC)

Figure 5 shows DSC thermograms of FB material, F14 pellet, sugar sphere, NaLS, HPMC E6, and physical mixture. DSC curve of FB, physical mixture and F14 pellet provided an endothermic peak at 81 °C, while no corresponding melting peaks was found for NaLS, HPMC E6, and sugar sphere. Additionally, the area of the peak from F14 pellet (equal to a heat of fusion of 9.37 J/g) was much smaller than those of physical mixture (equal to a heat of fusion of 14.77 J/g) and FB material (equal to a heat of fusion of 71.31 J/g). In general, PXRD and DSC results confirmed a partial transformation from the crystalline state of FB in FB material to amorphous state in F14 pellet.

3.2.3. Fourier-transform infrared spectroscopy (FT-IR)

Figure 6 illustrates FT-IR diagrams of FB material, F14 pellet, sugar sphere, NaLS and HPMC E6. The free drug produced the chief distinguishing spikes at approximately 1728 (C=O bond), 1600 (aromatic ring), and 765 (C-Cl bond) cm^{-1} (Robert M. Silverstein, 2014). These peaks also appeared on the spectrum of F14 pellet, indicating that F14 pellet was successfully layered with the drug. In addition, in terms of intensity, the peaks on F14 spectrum were significantly lower, probably indicating the interactions of FB with other components in the solid dispersion system. This finding was in line with PXRD and DSC data detailed above.

3.3. Stability of F14 pellets

Firstly, F14 pellets stored under the long-term condition for 12 months and under the accelerated condition for 1 month were investigated for FB content, dissolution rates, and sensory evaluation (Fig. 7). For the pellets under the accelerated condition, the FB dissolution profiles of stored pellets in 0.4% NaLS medium were similar with the initial profiles ($f_2=68.1$)

with no significant differences at 60-minute points (Fig.7A–B). Moreover, there was no change in shape and color of the test capsule during the storage period, and the content of FB also insignificantly reduced (Fig.7E). Similarly, the pellets under a long-term condition (12 months) also shared similar properties in comparison with those of initial pellets (Fig.7C–D, E). Then, possibility of transformation from amorphous state into crystalline state of FB in 12-month F14 pellets (Fig.4, Fig.5), molecular interactions of FB with other components (Fig.6), were determined using PXRD, DSC, and FT-IR, respectively. The physicochemical data, once again, indicated that FB in the stored pellets was still mainly in amorphous state in interacting with other components. Based on the results, F14 pellets not only remained stable within 1 month under the accelerated condition, but also in 12 months of storage under the long-term condition.

3.4. HPLC method validation

The developed HPLC method was validated by evaluating selectivity, carryover, linearity, LOD, LLOQ, recovery, precision, accuracy, and stability for both of FA and FB. Chromatograms in Figure 8 showed that FA, FB, and IS were separately elucidated over time using a gradient program for mobile phase (Table 2).

Linearity was confirmed over concentration ranges of 0.1–50 $\mu\text{g}/\text{mL}$ for FA ($r=0.998$) and 0.2–50 $\mu\text{g}/\text{mL}$ for FB ($r=0.993$). The LLOQs for the two compounds were 0.1 $\mu\text{g}/\text{mL}$ (FA) and 0.2 $\mu\text{g}/\text{mL}$ (FB) (Table 3). The extraction recoveries of the FA and FB across the concentrations ranged from $65.84 \pm 1.93\%$ to $72.52 \pm 5.15\%$ and from $70.81 \pm 5.89\%$ to $73.41 \pm 2.48\%$, respectively (Table 4). The extraction method also was reproducible with $\text{RSD} < 10\%$ (between 2.93% and 8.31%, data not shown). Also, the extraction efficiency of IS at a concentration was over 85% with high repeatability ($\text{RSD} < 5\%$) (data not shown). These results indicated that the LLE extraction method could extract FA, FB, and IS with quite high extraction efficiency and reproducibility.

The precision for the two compounds ranged from 1.7% to 8.6% within a single day, and from 5.6% to 8.6% over consecutive three days. Intra-day and inter-day accuracies for FA and FB were between 89.73% and 109.93% (Table 5). These data indicated that the method was precise. Also, obtained chromatograms revealed no cross-contamination between blank samples and standard samples (Fig. 8). For stability study, FA and FB were stable at different storage conditions: 6 hours at room temperature, 24 hours in autosampler (5 °C), 3 freeze-thaw cycles,

and 30 days at $-30\text{ }^{\circ}\text{C} \pm 5\text{ }^{\circ}\text{C}$ (Table 6). These results of the method validation, finally, satisfied Bioanalytical Method Validation Guidance for Industry of FDA (2018) (FDA, 2018), thus could be applied in further *in vivo* study.

3.5. *Pharmacokinetic and comparative bioavailability studies*

3.5.1. *Pharmacokinetic analysis*

After single oral administration of 160 mg FB, the plasma concentrations of FA were determined by the validated HPLC method. Chromatograms over time revealed that no unchanged FB was found in the plasma (Figure 8). This finding was also consistent with the reports from Li *et al.* and Hanafy *et al.* (Hanafy *et al.*, 2007; Li *et al.*, 2019). Figure 9 shows the mean plasma concentration profiles of reference product and test capsule. The major pharmacokinetic parameters such as AUC_{0-24} , $\text{AUC}_{0-\infty}$, C_{max} , T_{max} , and $t_{1/2}$ for the two products were provided in Table 7. The AUC_{0-24} of the test capsule was $20.71 \pm 11.17\text{ }\mu\text{g}\cdot\text{h}/\text{mL}$ and was not significantly different from that of the reference tablet ($18.94 \pm 9.34\text{ }\mu\text{g}\cdot\text{h}/\text{mL}$) (a *p*-value of 0.7052). Similarly, the C_{max} of the test capsule ($2.03 \pm 1.07\text{ }\mu\text{g}/\text{mL}$) was insignificantly different to that for the reference tablet ($1.85 \pm 0.74\text{ }\mu\text{g}/\text{mL}$) (a *p*-value of 0.6669). In line with significant dissolution profiles of two preparations (Figure 3A and Figure 3B). T_{max} of test product (2.28 ± 1.42 hours) was significantly shorter than the figure for reference product (4.75 ± 1.27 hours) with a *p*-value of 0.0007. The T_{max} for reference product found in this study was close to the report of Abbott, USA (from 4 to 5 hours) (EMA, 2016). In addition to the capacity of solid dispersion in enhancing dissolution rates of poorly water-soluble drugs, this phenomenon possibly comes from a rapid release upon dosing of small pellets in comparison with tablets with larger size. Also, narrow distribution of FB powder in the gastrointestinal upon disintegrating from tablets may trigger lower dissolution rates of FB in comparison with pellets (Patel and Gohel, 2019).

3.5.2. *Bioequivalence analysis*

Statistical data of the bioequivalence studies of the two preparations containing 160 mg of FB in experimental beagle dogs were provided in Table 8. In this present study, log-transformed data of AUC_{0-24} and C_{max} were used for measuring 90% CIs of the geometric mean ratios of test to reference. The calculated 90% CIs for AUC_{0-24} and C_{max} were 85.27%–109.64% and

82.91%–123.04%, respectively. The data satisfied the acceptance criteria of 80.00%–125.00% from EMC guidelines (EMA, 2010). Moreover, AUC_{0-24} and C_{max} of the test capsule and the reference tablet were insignificantly different. These results revealed that developed FB capsule was bioequivalent to reference product, Lipanthyl® 160 mg tablet.

There is, currently, a trend towards employing combinations of various approaches for solubility enhancement of poorly water-soluble active ingredients in pharmaceutical research and pharmaceutical industry, such as a blend of solid dispersions and nanoparticles or solid dispersions and self-nanoemulsifying (Eggenreich et al., 2016, Ibrahim et al., 2018, Piao et al., 2014). These combinations probably make the most of advantages of individual approach, and each approach also plays a role as complementary parts for the others as well like FB was formulated as nanosuspensions and later converted to tablets (Tricor®, Triglide®). With a rapid growth of pharmaceutical technologies, promising results in this study as a first step to not only develop solid dispersion-based capsules and tablets containing fenofibrate but also take advantages of solid dispersions and nanoparticles with the aim of producing commercial products.

4. Conclusion

In the present study, the results from PXRD and DSC measurement indicated that fenofibrate existed in amorphous form, and remained stable over a long-term condition for 12 months and an accelerated condition for 1 month. Pelletized solid dispersion enhanced the dissolution rates of FB and this resulted in the satisfaction of the immediate-released fenofibrate capsule in meeting the criteria on the dissolution rate in USP 38. In the bioequivalence study in experimental beagle dogs, no significant differences in pharmacokinetic parameters was found between the test capsule and the reference tablet as 90% CIs for AUC_{0-t} and C_{max} were within the regulatory acceptance criteria. In addition, the test capsules provided significantly shorter T_{max} compared to the figure for reference product. These results probably released the potential for prescribing the new FB formulation as an alternative to Lipanthyl® 160 mg tablet in the future.

Acknowledgements

This research is funded by the Vietnam National Foundation for Science and Technology Development (NAFOSTED) under grant number: 01/2018/TN.

Conflicts of Interest

The authors report no conflicts of interests. The authors alone are responsible for the content and writing of this article.

References

- Adkins, J.C., Faulds, D., 1997. Micronised fenofibrate: a review of its pharmacodynamic properties and clinical efficacy in the management of dyslipidaemia. *Drugs*. 54, 615-633.
- Alshamsan, A., Kazi, M., Badran, M.M., Alanazi, F.K., 2018. Role of Alternative Lipid Excipients in the Design of Self-Nanoemulsifying Formulations for Fenofibrate: Characterization, in vitro Dispersion, Digestion and ex vivo Gut Permeation Studies. *Front. Pharmacol.* 9, 1219.
- Baghel, S., Cathcart, H., O'Reilly, N.J., 2016. Polymeric Amorphous Solid Dispersions: A Review of Amorphization, Crystallization, Stabilization, Solid-State Characterization, and Aqueous Solubilization of Biopharmaceutical Classification System Class II Drugs. *J. Pharm. Sci.* 105, 2527-2544.
- Ballantyne, C.M., 2009. *Clinical lipidology: a companion to Braunwald's heart disease*. Elsevier Health Sciences.
- Eggenreich, K., Windhab, S., Schrank, S., Treffer, D., Juster, H., Steinbichler, G., Laske, S., Koscher, G., Roblegg, E., Khinast, J.G., 2016. Injection molding as a one-step process for the direct production of pharmaceutical dosage forms from primary powders. *Int. J. Pharm.* 505, 341-351.
- EMA, 2010. Guideline on the investigation of bioequivalence. 2010. Doc. Ref.: CPMP/EWP/QWP/1401/98 Rev.1. <https://www.ema.europa.eu/investigation-bioequivalence>. Access date: 23/04/2019
- EMA, 2016. Fenofibrate 160mg Tablets. <https://www.medicines.org.uk/emc/product/5267/smpe>. Access date: 23/04/2019.
- FDA, 2002. Guidance for Industry Bioavailability and Bioequivalence Studies for Orally Administered Drug Products — General Considerations, <https://www.fda.gov/downloads/Drugs/Guidances/ucm154838>. Access date: 23/04/2019.
- FDA, 2018. Bioanalytical Method Validation Guidance for Industry <https://www.fda.gov/downloads/Drugs/Guidances/ucm070107.pdf>. Access date: 23/04/2019.
- Fischer J., G.C.R., 2006. *Analogue-based Drug Discovery*. Wiley-VCH.

- Guichard, J.P., Blouquin, P., Qing, Y., 2000. A new formulation of fenofibrate: Suprabioavailable tablets. *Current Medical Research and Opinion* 16, 134-138.
- Hanafy, A., Spahn-Langguth, H., Vergnault, G., Grenier, P., Tubic Grozdanis, M., Lenhardt, T., Langguth, P., 2007. Pharmacokinetic evaluation of oral fenofibrate nanosuspensions and SLN in comparison to conventional suspensions of micronized drug. *Adv. Drug. Deliv. Rev.* 59, 419-426.
- Hens, B., Brouwers, J., Corsetti, M., Augustijns, P., 2015. Gastrointestinal behavior of nano- and microsized fenofibrate: In vivo evaluation in man and in vitro simulation by assessment of the permeation potential. *Eur. J. Pharm. Sci.* 77, 40-47.
- Ibrahim, A.H., Ibrahim, H.M., Ismael, H.R., Samy, A.M., 2018. Optimization and evaluation of lyophilized fenofibrate nanoparticles with enhanced oral bioavailability and efficacy. *Pharm. Dev. Technol.* 23, 358-369.
- Kumar, R., Siril, P.F., 2018. Enhancing the Solubility of Fenofibrate by Nanocrystal Formation and Encapsulation. *AAPS PharmSciTech.* 19, 284-292.
- Lalloyer, F., Staels, B., 2010. Fibrates, Glitazones, and Peroxisome Proliferator-Activated Receptors. *Arter. Thromb. Vasc. Biol.* 30, 894-899.
- Li, F., Zheng, X., Bao, Y., Chen, T., Zeng, J., Xu, X., Yan, C., Feng, L., 2019. Fenofibrate modified-release pellets with lag phase and high oral bioavailability. *Drug. Des. Devel. Ther.* 13, 141-151.
- Ling, H., Luoma, J.T., Hilleman, D., 2013. A Review of Currently Available Fenofibrate and Fenofibric Acid Formulations. *Cardiovasc Res.* 4, 47-55.
- Min, M.H., Park, J.H., Hur, J.H., Shin, H.C., Cho, Y., Kim, D.D., 2019. Formulation and bioequivalence studies of choline alfoscerate tablet comparing with soft gelatin capsule in healthy male volunteers. *Drug. Des. Devel. Ther.* 13, 1049-1058.
- Patel, H., Gohel, M., 2019. A review on enteric coated pellets composed of core pellets prepared by extrusion-spheronization. *Recent. Pat. Drug. Deliv. Formul.* DOI: 10.2174/1872211313666190212115139.
- Patki, M., Patel, K., 2019. Development of a solid supersaturated self-nanoemulsifying concentrate (S-superSNEP) of fenofibrate using dimethylacetamide and a novel co-processed excipient. *Drug Dev. Ind. Pharm.* 45, 405-414.
- Pestieau, A., Lebrun, S., Cahay, B., Brouwers, A., Streel, B., Cardot, J.M., Evrard, B., 2017. Evaluation of different in vitro dissolution tests based on level A in vitro-in vivo correlations for fenofibrate self-emulsifying lipid-based formulations. *Eur. J. Pharm. Biopharm.* 112, 18-29.

- Piao, Z.Z., Choe, J.S., Oh, K.T., Rhee, Y.S., Lee, B.J., 2014. Formulation and in vivo human bioavailability of dissolving tablets containing a self-nanoemulsifying itraconazole solid dispersion without precipitation in simulated gastrointestinal fluid. *Eur. J. Pharm. Sci.* 51, 67-74.
- Qiu, F., Meng, T., Chen, Q., Zhou, K., Shao, Y., Matlock, G., Ma, X., Wu, W., Du, Y., Wang, X., Deng, G., Ma, J.X., Xu, Q., 2019. Fenofibrate-Loaded Biodegradable Nanoparticles for the Treatment of Experimental Diabetic Retinopathy and Neovascular Age-Related Macular Degeneration. *Mol. Pharm.* DOI: 10.1021/acs.molpharmaceut.8b01319.
- Raymond C. Rowe, P.J.S., Marian E. Quinn, 2009. *Handbook of Pharmaceutical Excipients*, 6 ed. The Pharmaceutical Press, USA.
- Robert M. Silverstein, F.X.W., David J. Kiemle, David L. Bryce, 2014. *Spectrometric Identification of Organic Compounds*, 8 ed. John Wiley & Sons.
- Sheu, M.T., Yeh, C.M., Sokoloski, T.D., 1994. Characterization and Dissolution of Fenofibrate Solid Dispersion-Systems. *Int. J. Pharm.* 103, 137-146.
- Shi, N.Q., Wang, S.R., Zhang, Y., Huo, J.S., Wang, L.N., Cai, J.H., Li, Z.Q., Xiang, B., Qi, X.R., 2019. Hot melt extrusion technology for improved dissolution, solubility and "spring-parachute" processes of amorphous self-micellizing solid dispersions containing BCS II drugs indomethacin and fenofibrate: Profiles and mechanisms. *Eur. J. Pharm. Sci.* 130, 78-90.
- Shi, N.Q., Zhang, Y., Li, Y., Lai, H.W., Xiao, X., Feng, B., Qi, X.R., 2017. Self-micellizing solid dispersions enhance the properties and therapeutic potential of fenofibrate: Advantages, profiles and mechanisms. *Int. J. Pharm.* 528, 563-577.
- Singh, A., Worku, Z.A., Van den Mooter, G., 2011. Oral formulation strategies to improve solubility of poorly water-soluble drugs. *Expert Opin. Drug Deliv.* 8, 1361-1378.
- Sironi, D., Rosenberg, J., Bauer-Brandl, A., Brandl, M., 2017. Dynamic dissolution-/permeation-testing of nano- and microparticle formulations of fenofibrate. *Eur. J. Pharm. Sci.* 96, 20-27.
- Streel, B., Hubert, P., Ceccato, A., 2000. Determination of fenofibric acid in human plasma using automated solid-phase extraction coupled to liquid chromatography. *J. Chromatogr. B* 742, 391-400.
- Sunazuka, Y., Ueda, K., Higashi, K., Tanaka, Y., Moribe, K., 2018. Combined effects of the drug distribution and mucus diffusion properties of self-microemulsifying drug delivery systems on the oral absorption of fenofibrate. *Int. J. Pharm.* 546, 263-271.
- The United States Pharmacopeia (USP) and The National Formulary (NF). 2015. USP 38–NF 33.

- Ueda, K., Iwai, T., Sunazuka, Y., Chen, Z., Kato, N., Higashi, K., Moribe, K., 2019. Effect of molecular weight of hypromellose on mucin diffusion and oral absorption behavior of fenofibrate nanocrystal. *Int. J. Pharm.* DOI: 10.1016/j.ijpharm.2019.04.033.
- Vo, C.L.N., Park, C., Lee, B.J., 2013. Current trends and future perspectives of solid dispersions containing poorly water-soluble drugs. *Eur. J. Pharm. Biopharm.* 85, 799-813.
- Vogt, M., Kunath, K., Dressman, J.B., 2008. Dissolution enhancement of fenofibrate by micronization, cogrinding and spray-drying: Comparison with commercial preparations. *Eur. J. Pharm. Biopharm.* 68, 283-288.
- Wang, G.X., Guo, J.F., Meng, F.H., Song, X.M., Zhong, B.H., Zhao, Y.M., 2012. Development of a sensitive liquid chromatography/tandem mass spectrometry method for the determination of fenofibric acid in rat plasma. *Biomed. Chromatogr.* 26, 497-501.
- Weng, T., Qi, J., Lu, Y., Wang, K., Tian, Z., Hu, K., Yin, Z., Wu, W., 2014. The role of lipid-based nano delivery systems on oral bioavailability enhancement of fenofibrate, a BCS II drug: comparison with fast-release formulations. *J. Nanobiotechnology.* 12, 39.
- Xin, R., An, D., Li, Y., Fu, J., Huang, F., Zhu, Q., 2019. Fenofibrate improves vascular endothelial function in diabetic mice. *Biomed. Pharmacother.* 112, 108722.
- Zhu, T., Ansquer, J.C., Kelly, M.T., Sleep, D.J., Pradhan, R.S., 2010. Comparison of the Gastrointestinal Absorption and Bioavailability of Fenofibrate and Fenofibric Acid in Humans. *J. Clin. Pharmacol.* 50, 914-921.
- Zhu, W., Romanski, F.S., Meng, X., Mitra, S., Tomassone, M.S., 2011. Atomistic simulation study of surfactant and polymer interactions on the surface of a fenofibrate crystal. *Eur. J. Pharm. Sci.* 42, 452-461.

Figures and Table legends

Fig. 1. (A) Pelletization process characteristics for F1, F2, F3, and F4; (B) Dissolution profiles of FB formulations against time in 0.72% NaLS medium; (C) Dissolution profiles of FB formulations in 0.72% NaLS medium at the 60-minute point.

Fig. 2. Dissolution profiles of FB formulation in 0.4% NaLS medium against time (curves) and at the 60-minute point (bar charts).

Fig. 3. (A) Dissolution profiles of FB formulations in 0.4% NaLS medium against time; (B) Dissolution profiles of FB formulations in 0.4% NaLS medium at the 60-minute point; (C) Size distribution of F14 pellets.

Fig. 4. PXRD patterns of (1) 12-month F14 pellet, (2) NaLS, (3) F14 pellet, (4) sugar sphere, (5) HPMC E6, (6) FB.

Fig. 5. DSC thermograms of (1) 12-month F14 pellet, (2) F14 pellet, (3) physical mixture, (4) HPMC E6, (5) FB, (6) NaLS, (7) sugar sphere.

Fig. 6. FT-IR diagram of (1) 12-month F14 pellet, (2) F14 pellet, (3) NaLS, (4) sugar sphere, (5) HPMC E6, (6) FB.

Fig. 7. (A) Dissolution profiles of F14 pellets in 0.4% NaLS medium before and after 1 month of accelerated storage, (B) Dissolution rate (60-minute point) of F14 pellets in 0.4% NaLS medium before and after 1 month of accelerated storage, (C) Dissolution profiles of F14 pellets in 0.4% NaLS medium before and after 12 months of storage, (D) Dissolution rate (60-minute point) of F14 pellets in 0.4% NaLS medium before and after 12 months of storage, (E) Characteristics of F14 pellets before and after different conditions of storage.

Fig. 8. Representative HPLC chromatograms of (A) blank samples; (B) standard samples at LLOQ; (C) animal samples of test product before dosing; and (D) animal samples of test product at 2 hours after dosing.

Fig. 9. Pharmacokinetic profiles of Lipanthyl® 160 mg tablet and Test capsule (n=10).

Table 1: Formulations and layering procedures of FB pellets.

Table 2. Gradient program of HPLC method.

Table 3. Calibration curve, LOD and LLOQ of FA and FB (n = 6).

Table 4. Recovery (%) of FA and FB against concentration (n = 6).

Table 5. Intra-day and inter-day accuracy and precision of FA and FB (n = 6).

Table 6. Stability of FA and FB in plasma (n=6).

Table 7. Pharmacokinetic parameters (n=10).

Table 8. Statistical results of bioequivalence evaluation of test and reference formulation of fenofibrate 160 mg in experimental beagle dogs (n=10).

Journal Pre-proofs

Formulation	Fenofibrate (g)	Dichloromethane (mL)	Enthanol (mL)	Polymer (g)	Surfactant (g)	Second carrier (g)	Sugar cores (g)
F1	2.5	30	30	HPMC E6: 2.5	-	-	5
F2	2.5	30	30	PVP K30: 2.5	-	-	5
F3	2.5	30	30	PEG 6000: 2.5	-	-	5
F4	2.5	30	30	Eudragit® EPO: 2.5	-	-	5
F5	2.5	30	30	HPMC E6: 1.25	-	-	5
F6	2.5	30	30	HPMC E6: 3.75	-	-	5
F7	2.5	30	30	HPMC E6: 5.00	-	-	5
F8	2.5	30	30	HPMC E6: 2.5	NaLS: 0.25	-	5
F9	2.5	30	30	HPMC E6: 2.5	NaLS: 0.5	-	5
F10	2.5	30	30	HPMC E6: 2.5	NaLS: 0.75	-	5
F11	2.5	30	30	HPMC E6: 2.5	NaLS:1.25	-	5
F12	2.5	30	30	HPMC E6: 2.5	NaLS: 2.5	-	5
F13	2.5	30	30	HPMC E6: 2.5	NaLS: 0.5	Poloxamer 407: 0.25	5
F14	2.5	30	30	HPMC E6: 2.5	NaLS: 0.5	HPMC E15: 0.25	5
F15	2.5	30	30	HPMC E6: 2.5	NaLS: 0.5	Tween 80: 0.25	5
F16	2.5	30	30	HPMC E6: 2.5	NaLS: 0.5	Span 60: 0.25	5
F17	2.5	30	30	HPMC E6: 2.5	NaLS: 0.5	PEG 4000: 0.25	5
F18	2.5	30	30	HPMC E6: 2.5	NaLS: 0.5	HPMC E15: 0.5	5
F19	30	360	360	HPMC E6: 30	NaLS: 6	HPMC E15: 3	20

Layering process parameters	Inlet air temperature (°C)	Product temperature (°C)	Air flow (m ³ /h)	Atomizing air pressure (bar)	Rate of layering (mL/h)	Nozzle port size (mm)	Filter shake interval (s)
Value	50	40	25-30	1.2	60	0.5	5

Abbreviations: HPMC, hydroxypropyl methylcellulose; PVP, polyvinyl pyrrolidone K30; PEG, polyethylene glycol; NaLS, sodium lauryl sulfate.

Table 1: Formulations and layering procedures of FB pellets.

Table 2. Gradient program of HPLC method.

Time (min)	MeOH:0.01M phosphate buffer pH 3.0
0→12.5	70: 30→ 90: 10
12.5→13.5	90: 10→ 70: 30

MeOH: methanol

Table 3. Calibration curve, LOD and LLOQ of FA and FB (n = 6).

Analyte	Regression equation	r	Range ($\mu\text{g/mL}$)	LOD ($\mu\text{g/mL}$)	LLOQ ($\mu\text{g/mL}$)
FA	$y = 0.133x + 0.009$	0.998	0.1 – 50	0.06	0.1
FB	$y = 0.101x - 0.003$	0.993	0.2 – 50	0.12	0.2

y: the peak area ratio of analyte to IS, diclofenac sodium.

x: corresponding concentration of analyte.

r: correlation coefficient.

Table 4. Recovery (%) of FA and FB against concentration (n = 6).

FA			FB		
Concentration (µg/mL)	Recovery ^a (%)	RSD (%)	Concentration (µg/mL)	Recovery ^a (%)	RSD (%)
0.2	65.84	2.93	0.5	73.41	2.48
40	72.52	7.10	40	70.81	8.31

^a Data is presented as mean value.

Table 5. Intra-day and inter-day accuracy and precision of FA and FB (n = 6).

Analyte	Intra-day				Inter-day		
	Conc. ($\mu\text{g/mL}$)	Found ^a ($\mu\text{g/mL}$)	Accuracy ^a (%)	RSD (%)	Found ^a ($\mu\text{g/mL}$)	Accuracy ^a (%)	RSD (%)
FA	0.2	0.23	102.80	6.1	0.23	101.37	6.1
	25	26.3	92.93	5.7	27.6	97.83	6.7
	40	42.3	93.58	2.4	44.1	97.56	6.0
FB	0.5	0.45	89.73	2.9	0.48	95.03	8.6
	25	27.5	109.93	1.7	26.9	107.47	5.6
	40	40.2	101.88	8.6	40.5	101.17	7.5

^a Data is presented as mean value.

Table 6. Stability of FA and FB in plasma (n=6).

Analyte	Spiked ($\mu\text{g/mL}$)	Freshly ($\mu\text{g/mL}$)	Room temperature		5 °C		freeze-thaw		-30 °C \pm 5 °C	
			6 hours	CV (%)	24 hours	CV (%)	3 cycles	CV (%)	30 days	CV (%)
FA	0.2	0.23 \pm 0.02	0.23 \pm 0.01	-1.7	0.23 \pm 0.01	-1.7	0.21 \pm 0.01	-8.9	0.25 \pm 0.01	5.2
	40	42.3 \pm 1.03	43.13 \pm 1.94	2	42.12 \pm 1.26	-0.4	40.05 \pm 2.24	-5.6	45.33 \pm 1.37	6.7
FB	0.5	0.45 \pm 0.01	0.48 \pm 0.04	6.7	0.45 \pm 0.05	-0.4	0.50 \pm 0.04	-6	0.53 \pm 0.01	-0.3
	40	40.73 \pm 3.52	41.65 \pm 2.59	2.3	41.50 \pm 3.17	1.9	39.03 \pm 1.28	0.34	35.68 \pm 1.37	-9

Each value represents the means \pm SD of three determinations.

Freshly: initial concentration of analytes.

6 hours: concentration of analytes after 6 hours at room temperature.

24 hours: concentration of analytes after 24 hours at 5 °C.

3 cycles: concentration of analytes after 3 cycles of freeze-thaw.

30 days: concentration of analytes after 30 days hours at -30 °C \pm 5 °C.

Table 7. Pharmacokinetic parameters (n=10).

Pharmacokinetic parameters	Lipanthyl® 160 mg tablet	Test capsule
AUC ₀₋₂₄ (µg×h/mL)	18.94 ± 9.34	20.71 ± 11.17
AUC _{0-∞} (µg×h/mL)	30.25 ± 12.81	33.28 ± 16.07
C _{max} (µg/mL)	1.85 ± 0.74	2.03 ± 1.07
T _{max} (hr)	4.75 ± 1.27	2.28 ± 1.42
t _{1/2} (hr)	12.26 ± 7.18	17.40 ± 14.78
R.B. (%)	100	108.55

Each value represents the means ± SD of three determinations.

AUC_{0-∞}: area under the curve extrapolated to infinity

AUC₀₋₂₄: area under the curve to the last measurable concentration

C_{max}: peak plasma concentration

T_{max}: time to peak concentration

t_{1/2}: half-life.

R.B.: relative bioavailability (AUC₀₋₂₄) to reference.

Oral dose= 160 mg.

Table 8. Statistical results of bioequivalence evaluation of test and reference formulation of fenofibrate 160 mg in experimental beagle dogs (n=10).

Parameter	Geometric mean		90% CI
	Test capsule	Lipanthyl® 160 mg tablet	
AUC ₀₋₂₄ (µg×h/mL)	19.28	18.43	85.27%–109.64%
C _{max} (µg/mL)	1.78	1.63	82.91%–123.04%

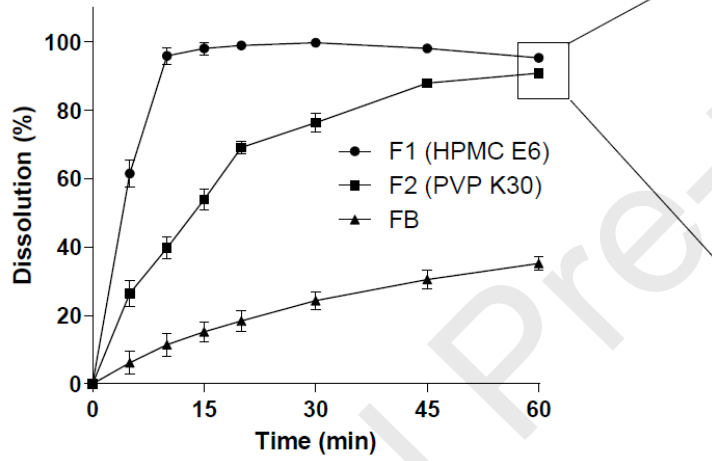
Figure 1

A

Formulation	Pellet process problem	Selection	Layering efficiency' (%)
F1	No issue	Selected	71.8
F2	Slightly sticking	Selected	47.4
F3	Filter blocking	Not selected	
F4	Very sticking	Not selected	
	Nozzle blocking		

* Data is mean value.

B



C

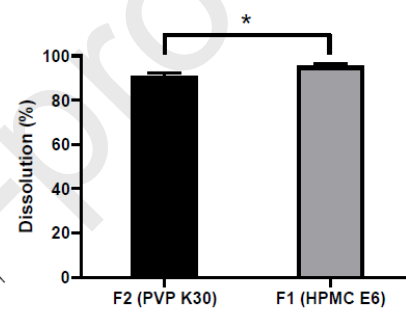
* $p = 0.01$

Figure 2

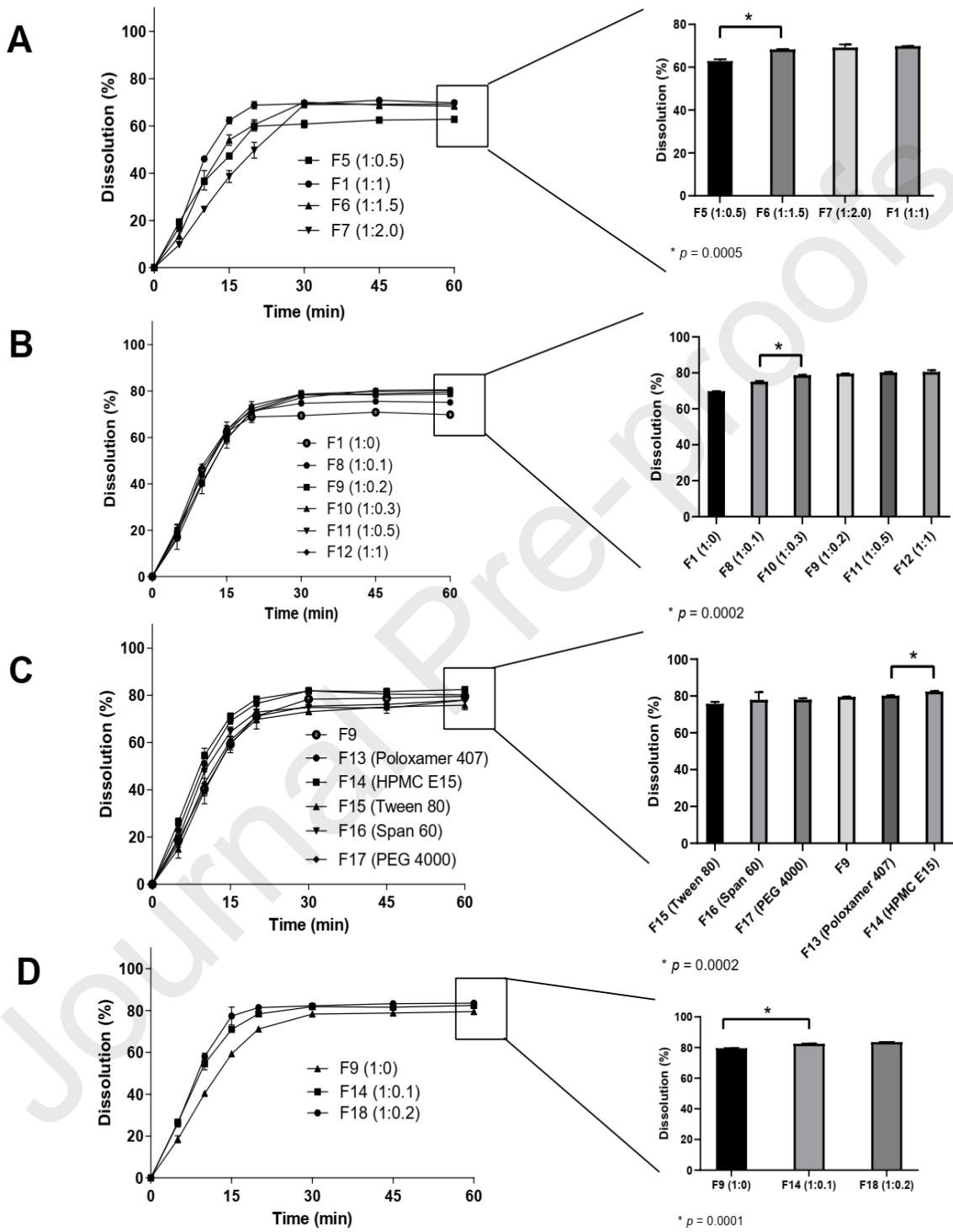
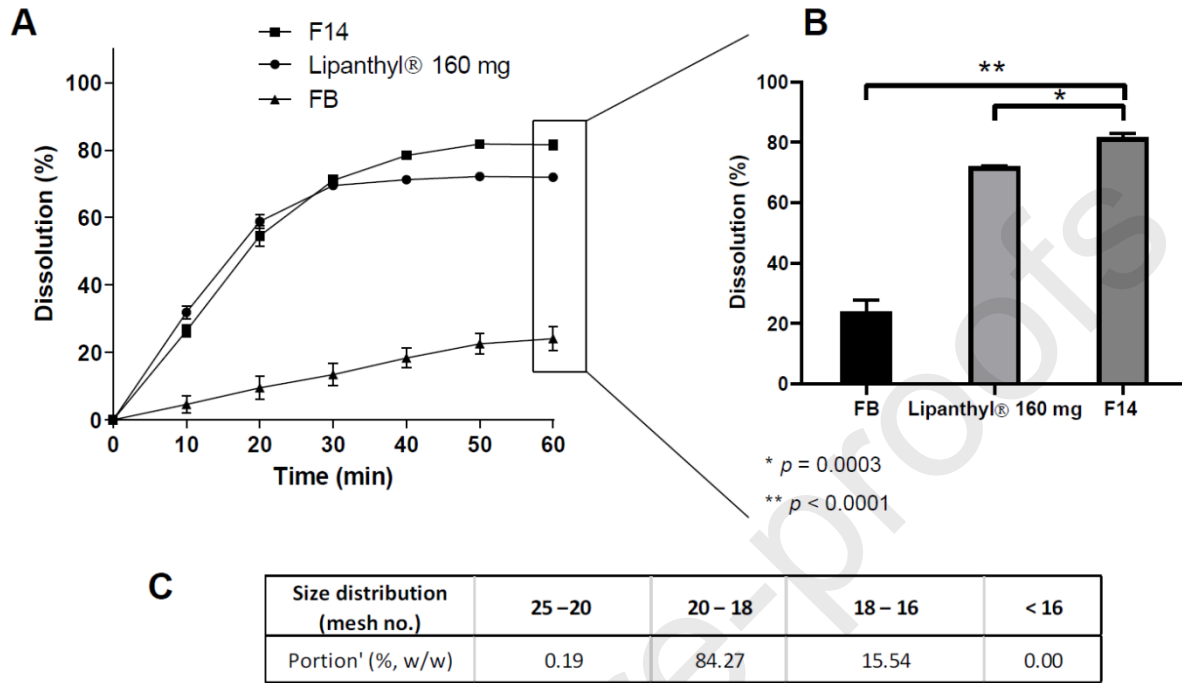


Figure 3



' Data is mean value.

Figure 4

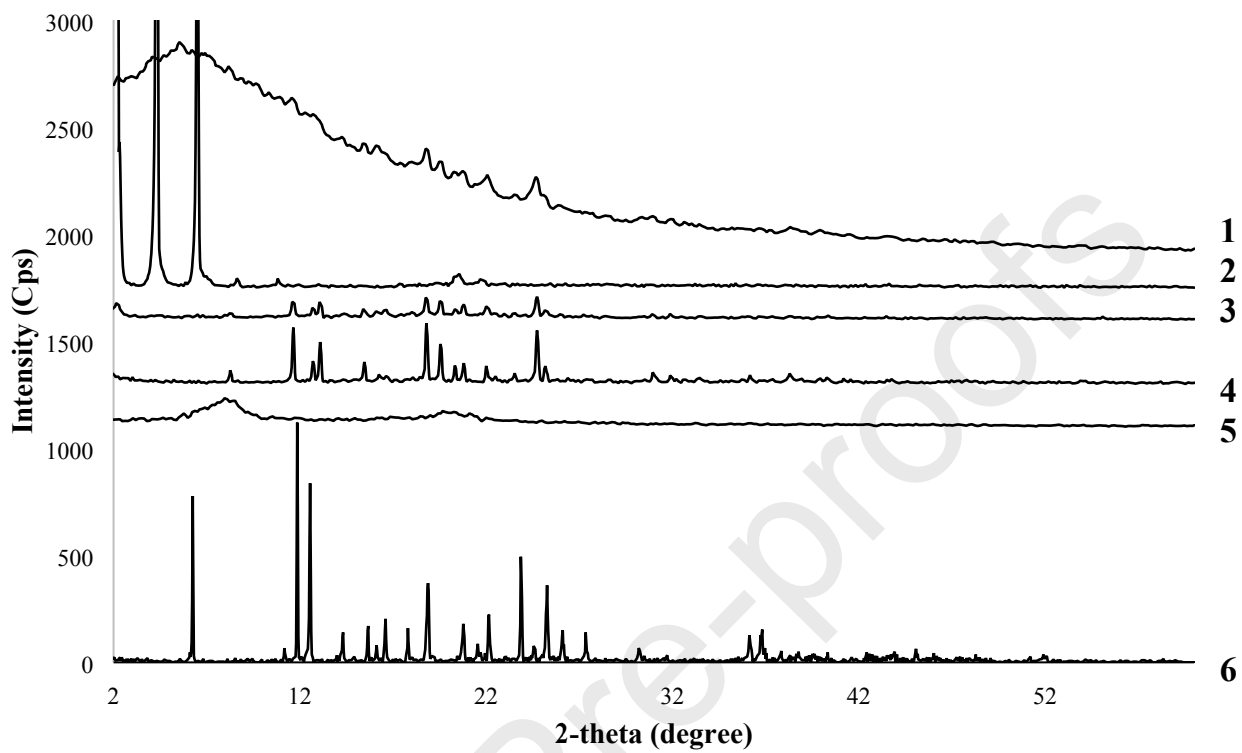


Figure 5

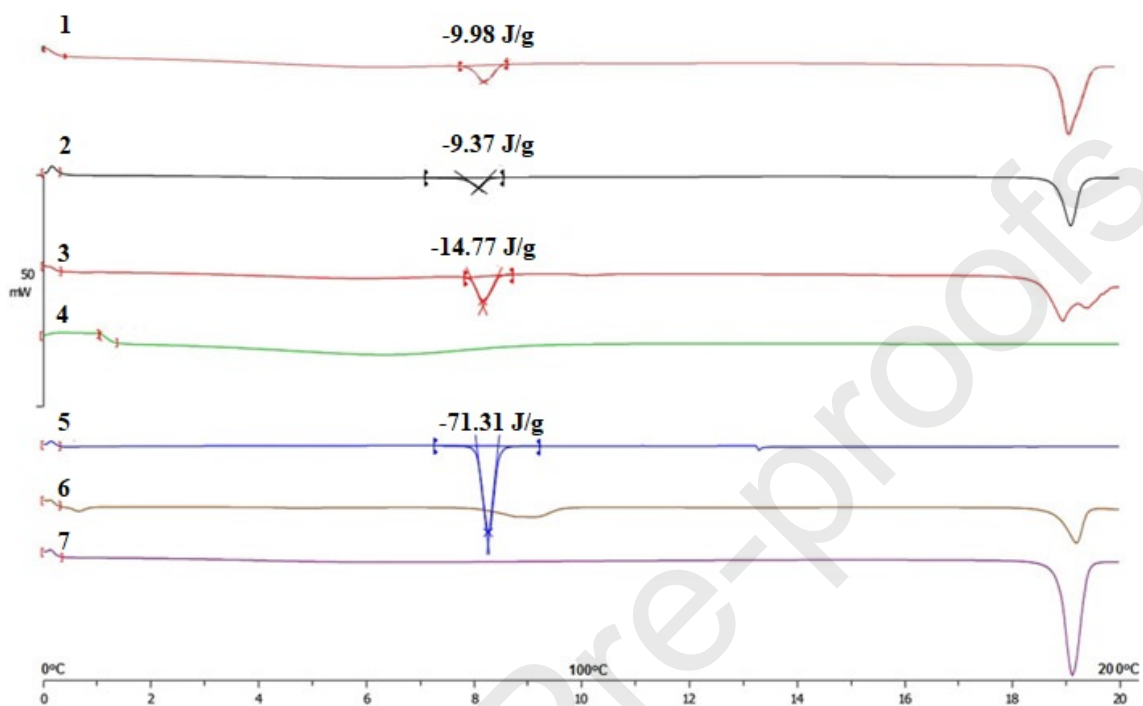


Figure 6

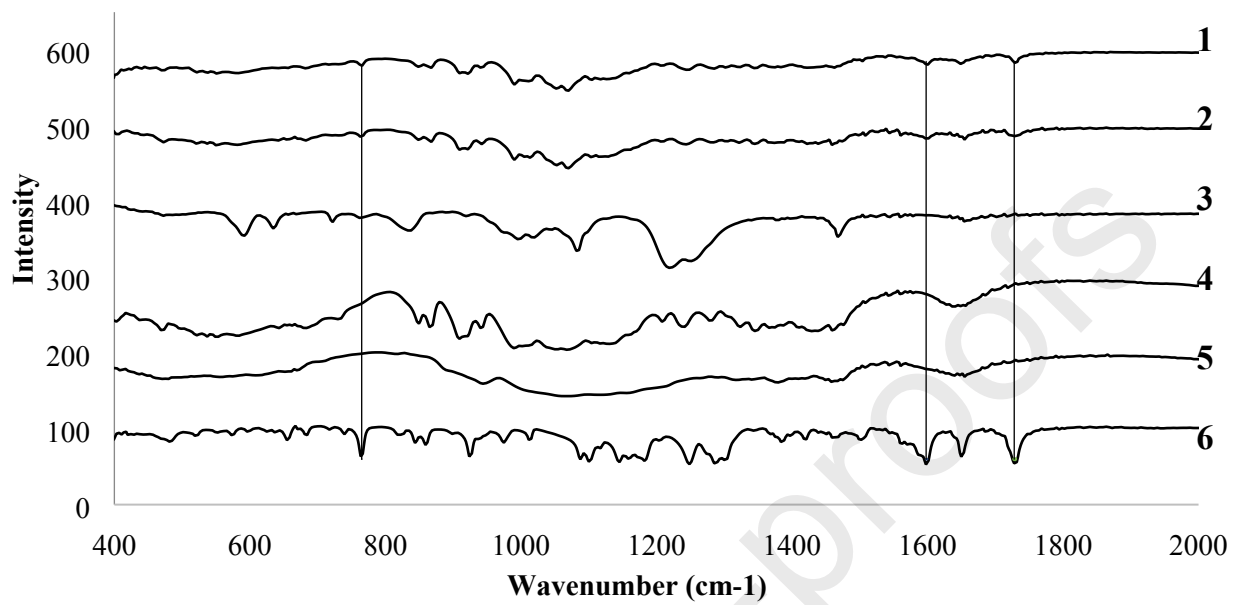
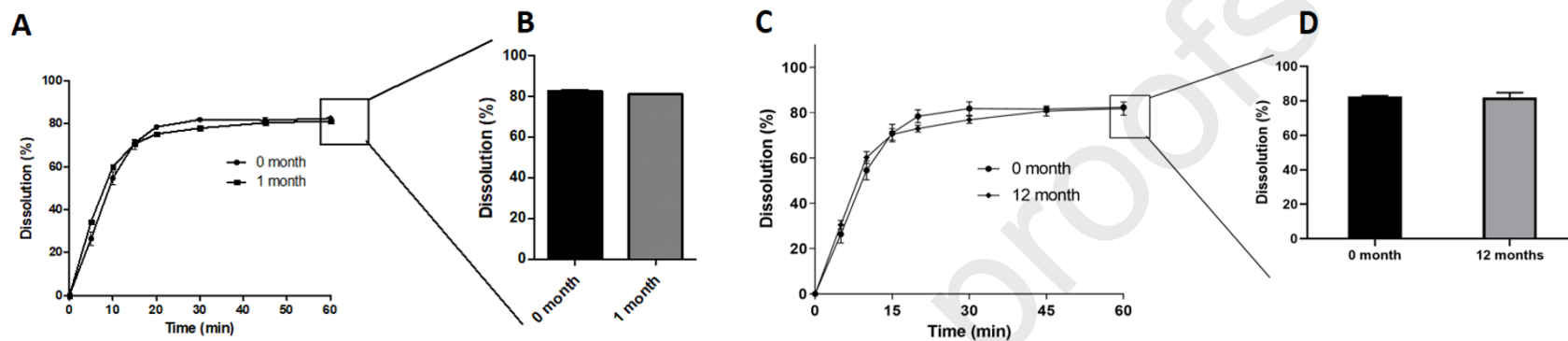


Figure 7



Month	0	1	12
Storage condition		40 °C ± 2 °C/75% RH ± 5% RH	30 °C ± 2 °C/75% RH ± 5% RH
Shape	Spherical and smooth uniformity	Spherical and smooth uniformity	Spherical and smooth uniformity
Color	Light yellow	Light yellow	Light yellow
Content ^a (%)	100	99.71	98.92
f ₂ ^a		68.1	70.1

RH: relative humidity

^a Stored pellets compared to initial pellets (0 month)

Figure 8

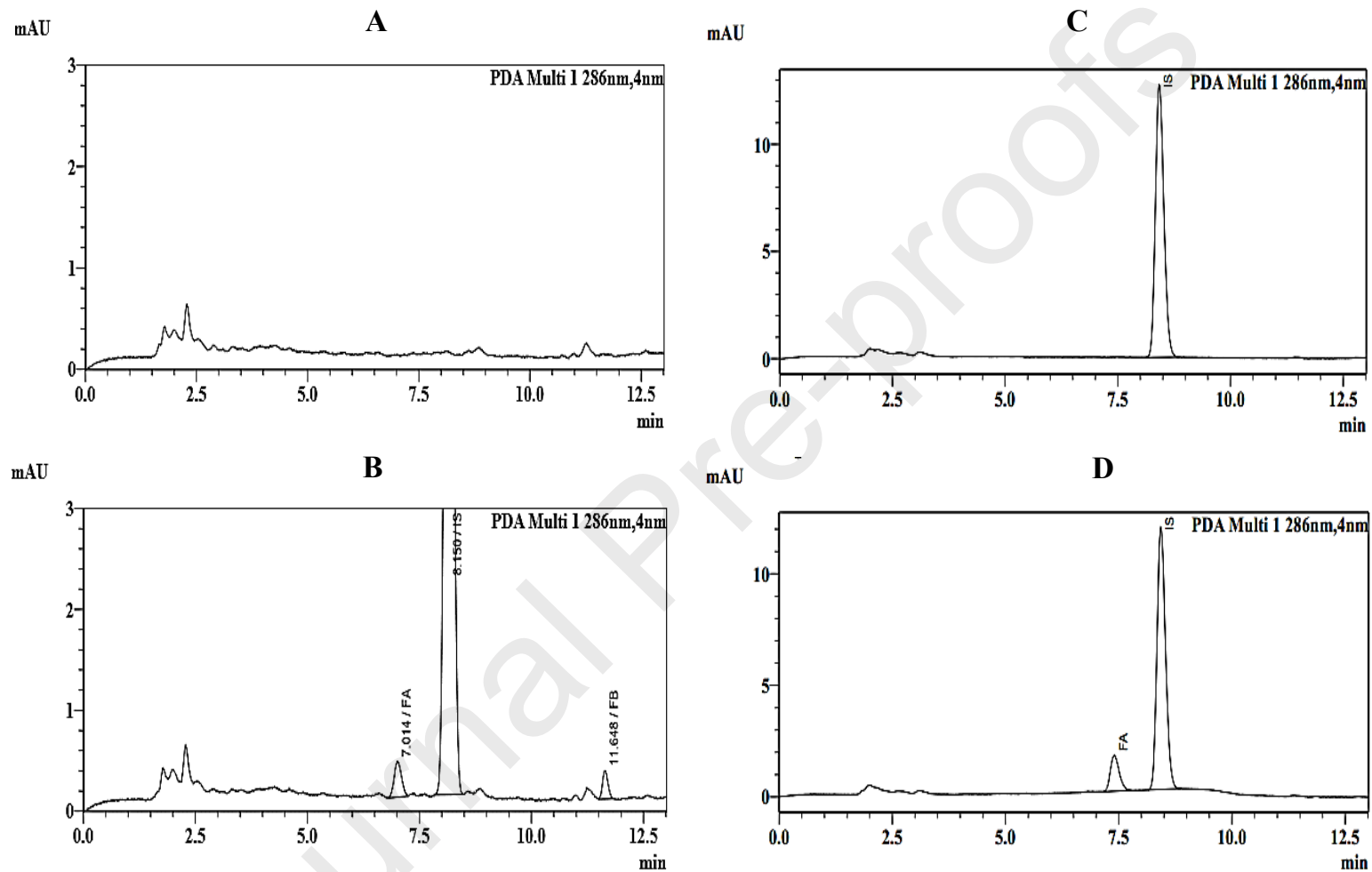
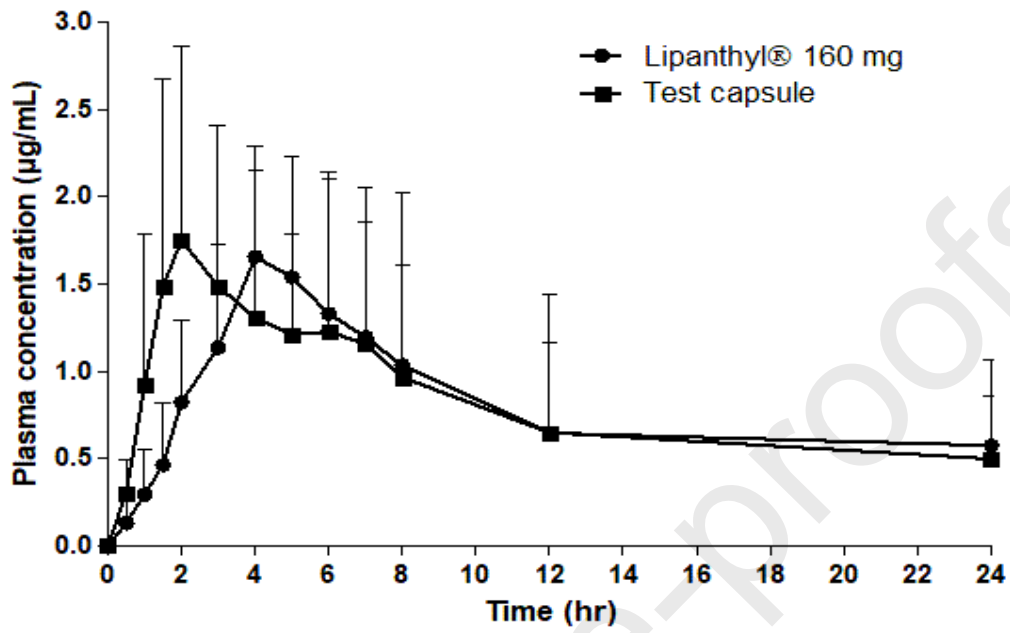


Figure 9



Declaration of interests

The authors declare that they have no known competing financial interests or personal relationships that could have appeared to influence the work reported in this paper.

Conflicts of Interest

The authors report no conflicts of interests. The authors alone are responsible for the content and writing of this article.